

PROCEEDINGS OF SPIE

SPIDigitalLibrary.org/conference-proceedings-of-spie

Comparing the accuracy of intraoral scanners, using advanced micro computed tomography

Mattia Sacher, Georg Schulz, Hans Deyhle, Kurt Jäger, Bert Müller

Mattia Sacher, Georg Schulz, Hans Deyhle, Kurt Jäger, Bert Müller, "Comparing the accuracy of intraoral scanners, using advanced micro computed tomography," Proc. SPIE 11113, Developments in X-Ray Tomography XII, 111131Q (10 September 2019); doi: 10.1117/12.2530728

SPIE.

Event: SPIE Optical Engineering + Applications, 2019, San Diego, California, United States

Comparing the accuracy of intraoral scanners, using advanced micro computed tomography

Mattia Sacher^{a,b}, Georg Schulz^a, Hans Deyhle^{a,c}, Kurt Jäger^{*a,d}, and Bert Müller^a

^aBiomaterials Science Center, Department of Biomedical Engineering, University of Basel, 4123 Allschwil, Switzerland; ^bPraxis-Team St. Margarethen Binningen, 4102 Binningen, Switzerland; ^cDiamond Light Source, Harwell Science and Innovation Campus, Didcot, Oxfordshire, OX11 0DE, United Kingdom; ^dPraxis-Team St. Margarethen AG, 4663 Aarburg, Switzerland

ABSTRACT

Intraoral scanners have been gaining importance in dental offices. The technology has become a valuable and economically reasonable alternative to conventional silicone impressions and conventional plaster casts, due to reduced treatment times and sufficient precision, which, for dental prostheses, depends on clinical needs. For the production of working models, tolerable inaccuracy is relatively generous, but especially for crowns, bridges and larger dental prostheses, which include several teeth over the dental arch, extra work is often performed – presumably caused by the limited accuracy of intraoral scanners. Therefore, this paper deals with the detailed evaluation of selected, commercially available intraoral scanner systems. For this purpose, we have designed and realized a model of the full arch upper jaw on the basis of clinically relevant imaging data. As well-defined references, we have incorporated cylinders with a diameter of 4 mm. This standard, to be used as a reference, was quantitatively characterized by four independent measurements using the advanced CT-system phoenix|x-ray nanotom[®] m (GE Sensing & Inspection Technologies GmbH, Wunstorf, Germany) with a pixel size of 35 μm . The standard was also scanned by using five commercially available intraoral scanners. In order to compare the accuracy of the ten measurements per scanner, the data were matched to the standard and their displacements were made visible with GOM Inspect (GOM GmbH Braunschweig, Germany). Applying the same approach, we analyzed the accuracy of two three-dimensionally printed dental models with the stereolithography printers Form 2, Formlabs Inc., Somerville MA, USA). The results demonstrate the currently possible levels of precision for selected intraoral scanners. They differ, however, not only in terms of necessary scanning time and ease of handling, but also in reachable accuracy. GOM Inspect provided the following precision values: TRIOS[®] 3 – 35 μm , CS 3600 – 43 μm and 3M[™] True Definition Scanner – 46 μm . The other two systems yielded less precise data: Medit i500 – 93 μm and Emerald[™] – 97 μm . The combination of advanced conventional microCT and adequate software for quantitative analysis permits a detailed evaluation of the performance of currently available intraoral scanners.

Keywords: Intraoral scanner, stereolithography printer, three-dimensional accuracy evaluation, advanced high-resolution tomography, microCT, full-arch scanning, registration, deviation field

1. INTRODUCTION

An increasing number of dental treatments require the highly precise impression of the oral situation, and the quality of the treatment, and the related success of the therapy depends on the correctly performed impression. For any fixed and removable prosthetics, the impression is fundamental, whilst for less critical cases, irreversible hydrocolloid materials, such as alginate, are used in conventional workflow. With an accuracy below 150 μm , these impressions are usually less precise than digital impressions [1]; however conventional impressions, taken with rigid trays and elastomeric materials, are so accurate that they are considered as the gold standard [2]. Conventional impressions require the production of a plaster cast model.

*kurt.jaeger@unibas.ch; phone +41 61 207 5431; fax 41 61 207 5499; www.bmc.unibas.ch

Developments in X-Ray Tomography XII, edited by Bert Müller,
Ge Wang, Proc. of SPIE Vol. 11113, 111131Q · © 2019 SPIE
CCC code: 0277-786X/19/\$21 · doi: 10.1117/12.2530728

In the digital workflow, no cast is needed, but depending on the procedure, a physical model with the necessary accuracy requirements has to be produced. These models are mostly three-dimensionally printed using stereolithography apparatuses (SLA), and they feature clinically acceptable accuracy [3]. Intraoral scanners (IOS) are gaining importance in dental offices, and so they are therefore responsible for a paradigm shift in prosthetic dentistry [2]. The latest generation of video-based systems (IOS) seem to be more accurate, faster and more efficient in clinical application than previously employed devices, and they are even suitable for less experienced practitioners, because of their simplified handling [1, 4, 5]. Intraoral scanners offer advantages compared to conventional impressions, and digital impressions are time-efficient and much more comfortable for patients. In particular, patients suffering from the gag reflex benefit [6].

Crowns and bridges can be directly manufactured using CAD/CAM, or, alternatively, models can be produced by means of stereolithography [7, 8]. The main disadvantages of IOS are acquisition costs and intricate access to light-tight areas, including sub-gingival preparations.

The technology involved in intraoral scanning has significantly improved since 1980, when the first CEREC was introduced to the market [9]. In the meantime, intraoral scanning has been established in a wide range of indications [10]. Intraoral scans are used in prosthodontics for inlays/onlays, crowns, frameworks, fixed and removable partial prostheses, posts and cores, crowns and bridges and for digital smile design. In orthodontics, digital impressions serve as the basis for treatment planning, for custom-made devices and aligners [11]. In implant surgery, intraoral scans are integrated into the digital workflow to plan clinical cases and produce surgical guides [12], and they are increasingly considered more often as highly accurate, exhibiting no difference in comparison to conventional impressions for crowns and fixed dental prostheses of limited length [13, 14]. In the current literature, however, long-spanning fixed restorations or totally removable prostheses, which include six or more elements, are deemed somewhat problematic [1, 11]. The available studies about the precision of IOS hardly cover the latest generation of devices. The progress in technology by comprising high-resolution cameras for data acquisition and high-performance software for the polygonal mesh generation of the model has led to sudden improvement of the IOS performance [15]. The advancement of software particularly has enabled solutions not otherwise possible with conventional impression technology. Here, it is possible not only to analyze imaging data in detail, but also to modify crown preparations during treatment. Potential deficiency in the obtained impressions can be minimized or even fully removed, and related shade measurements assist in the determination of crown color. In order to educate the patient, the captured images can be presented immediately after scanning, while a series of scans from the same patient can be the basis of monitoring changes over time.

The aim of this study is the precision analysis of five recently introduced IOS systems on one milled master model across the span of a maxillary full denture, using advanced hard X-ray tomographic imaging.

2. METHODOLOGY

2.1 Model fabrication

The anatomic model of a maxillary full denture, based on standard working models (frasaco GmbH, Tettngang, Germany), was created with computer-assisted design (CAD) and commercially available software (Meshmixer, Autodesk Inc., San Rafael CA, USA). The parallel cylinders, with a pre-defined inner diameter and a depth of 4 mm, were placed at tooth positions 17 (C1), 21 (C2) and 27 (C3) as reference elements (see photograph in Figure 1). A characteristic crown preparation at tooth 23, and an inlay preparation at tooth 16, simulated a normal prosthetic situation. The master model was milled out of an industrially manufactured polyetheretherketone (PEEK) block (Denseo PEEK blank, Denseo GmbH, Aschaffenburg, Germany) on a five-axis computerized-numerical-control (CNC) milling machine (SilaMill 5, vhf camfacture AG, Ammerbuch, Germany). PEEK is a high-performance polymer, and it is known to be dimensionally stable [16] and is also used in medical applications (see e.g. [17]). An extension on the back of the model served for mounting purposes.

In addition, two other models were fabricated using the same design. A photopolymer resin, namely Dental Model Resin (Formlabs, Somerville MA, USA), was used within the SLA printers Form 2 (Formlabs, Somerville MA, USA) and

with a layer thickness of 25 μm . Models fabricated by the stereolithography technology were washed with isopropyl alcohol for a period of 15 minutes. Subsequently, they were post-cured with UV light under an inert gas atmosphere. The density of the models was experimentally determined to 1.59 g/cm^3 , which is significantly higher than the value of the raw material at 1.12 g/cm^3 . This result is an indicator of cross-linking at the 405 nm wavelength.

2.2 Reference generation

The microCT scans of the master model, described above, served as reference data. Tomographic data were recorded using the advanced conventional system nanotom[®] m (phoenix|x-ray, GE Sensing & Inspection Technologies GmbH, Wunstorf, Germany), as shown in Figure 1. This system is equipped with a nanofocus tube with a maximal acceleration voltage of 180 kV, which produces power of up to 15 W. For data acquisition, we employed the maximal acceleration voltage and a beam current of 30 μA . In order to shift the mean photon energy to higher values, a 0.5 mm-thin copper film was placed behind the transmission target. We recorded 1,600 radiographs throughout 360°. The exposure time for the first two datasets was set to 3 s per radiograph, whereas it was increased to 9 s for the third and to 24 s for the fourth dataset. In order to investigate the repeatability of the microCT-system and the impact of the cone beam, the following source-sample distances (SSDs) and source-detector distances (SDDs) were positioned. For the first and the second scans, SSD and SDD, were 78.75 and 225.00 mm, respectively. For the third scan, we used SSD 157.50 mm and SDD 450.00 mm, and for the fourth scan SSD 210.00 mm and SDD 600.00 mm were used. Exposure times were adapted to maintain comparable intensities, and the effective pixel length corresponded to 35 μm .

For visualization purposes, the acquired volume data were processed by means of VGStudio MAX (Volume Graphics, Heidelberg, Germany). In addition, the data size was reduced and converted into the standard triangulation language (STL) format. This conversion enabled us to compare the tomography data with data for the intraoral scans.

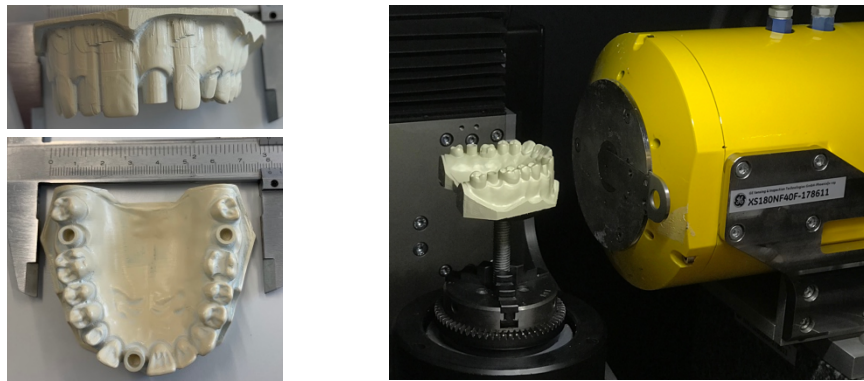


Figure 1. The PEEK model's size corresponds to that found in the human body, as displayed by the photographs on the left. Three well-defined hollow cylinders were incorporated to determine the precision of the intraoral scanners. The other photograph shows the placement of the model on the rotation stage in the CT-system nanotom[®] m (phoenix|x-ray, GE Sensing & Inspection Technologies GmbH, Wunstorf, Germany).

2.3 Data acquisition, using intraoral scanners

This study comprises five IOS systems, namely the 3M[™] True Definition Scanner (3M ESPE, St. Paul MN, USA), the TRIOS[®] 3 (3shape, Copenhagen, Denmark), the CS 3600 (Carestream, Atlanta GA, USA), the Medit i500 (Medit corp., Seongbuk-gu, South Korea) and the Emerald[™] (Planmeca Oy, Helsinki, Finland). With each system, the master model was scanned ten times, to obtain the necessary statistics. For this purpose, the model was mounted in the anatomically correct upright position. One trained examiner (M.S.) performed all of the scans in identical conditions (light, temperature, etc.), and scanner handling, the use of powder and the scan path were carried out according to the manufacturer's guidelines. 3M recommended the use of powder to improve the scanning results. To prepare the model as recommended, a thin layer of powder (3M Powder Sprayer; 3M, St. Paul, USA) was applied to the model. The scans with the other four systems were taken without the application of powder, i.e. in a powder-free fashion.

2.4 Data procession and evaluation

The measurements and analyses were performed using the well-established software GOM Inspect (GOM GmbH, Braunschweig, Germany). The positions of the three hollow cylinders were determined using their center points, identified via the Gaussian best-fit method (see Figure 2). The three distances were derived from tomography and IOS data individually (see Figure 3).

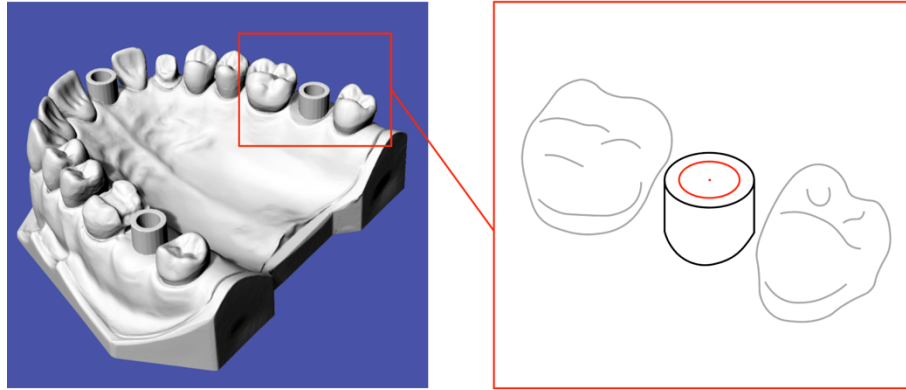


Figure 2. Scheme for determining the center points of the hollow cylinders via the Gaussian best-fit method.

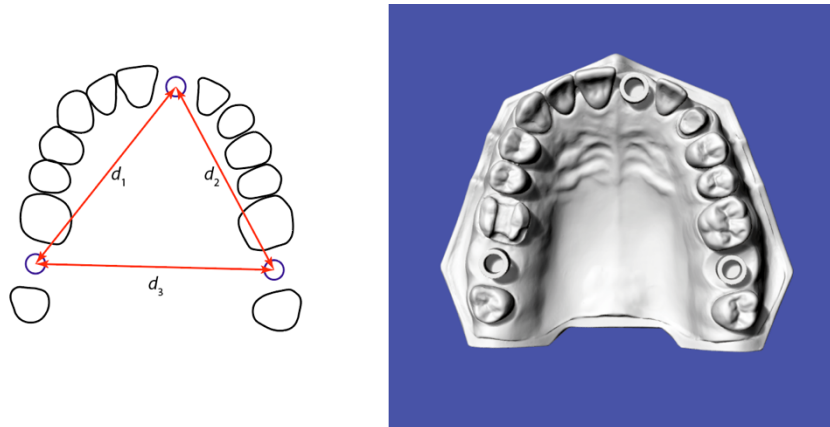


Figure 3. Scheme for specifying the three distances. Distance d_1 characterizes the length between 17 and 21, distance d_2 is the length between 21 and 27 and distance d_3 corresponds to the length between 21 and 27.

In order to compare accuracy (trueness and precision), these data were matched to the reference. The global best-fit deviation was calculated for each scan, in order to visualize the displacement field (see below).

3. RESULTS AND DISCUSSION

3.1 Measurements with nanotom[®] m

In order to confirm the well-known stability of the microCT-system and the reproducibility of the tomographic data acquisition, the first two scans were performed in identical conditions. As expected, differences were within the micrometer range, and even for distances between 4 and 5 cm, as given by the spacing between the hollow cylinders, the differences were well below the voxel length of $35\ \mu\text{m}$. For Scan 1, we found $d_1 = 45.444\ \text{mm}$, $d_2 = 41.622\ \text{mm}$, and $d_3 = 48.098\ \text{mm}$. For Scan 2, the selected distances were determined to $d_1 = 45.450\ \text{mm}$, $d_2 = 41.627\ \text{mm}$, and $d_3 = 48.101\ \text{mm}$. This result, i.e. differences of $4\text{-}6\ \mu\text{m}$ or relative deviations by about 10^{-4} , indicates that imaging modality and the method for

determining longitude are appropriate choices for precision measurements. As a consequence, we assumed an error bar of $6\ \mu\text{m}$ for establishing the spacing between the hollow cylinders.

In order to evaluate the impact of the cone beam geometry in the nanotom[®] m on the precision measurements, two scans with modified sample positions with respect to source and detector were performed. The experimentally determined distances between the hollow cylinders of Scan 3 were $d_1 = 45.468\ \text{mm}$, $d_2 = 41.640\ \text{mm}$, and $d_3 = 48.127\ \text{mm}$. The values for Scan 4 amounted to $d_1 = 45.480\ \text{mm}$, $d_2 = 41.647\ \text{mm}$, and $d_3 = 48.134\ \text{mm}$. Compared to the set value, given by the STL file ($d_1 = 45.503\ \text{mm}$, $d_2 = 41.676\ \text{mm}$, and $d_3 = 48.192\ \text{mm}$), we identified values only 23, 29, and 58 μm smaller. Although the discrepancies amount only to one-tenth of a percent and less than two pixel lengths, the phenomenon was still detectable. Therefore, tomographic data acquisition for the three-dimensionally printed models was performed with the parameters in Scan 4. It should be noted, however, that the potential gain in precision meant that data acquisition took seven times longer to complete than the standard approach.

3.2 Geometry of the PEEK model

The PEEK model was generated from the STL data by a milling machine, so it therefore unknown how far the model corresponds to the desired geometry. Comparing the STL data with the tomography data, one obtains a superposition of deficiencies from milling and imaging. Previous studies with the nanotom[®] m, however, demonstrate true micrometer precision, which is further supported by the measurements described above. Therefore, we can reasonably estimate the precision of the PEEK machining through a direct comparison of STL data with high-resolution tomography data.

Figure 4 elucidates the differences between the design data, with the measured ones using the color code on the color bar. The red color indicates positions where material more than $100\ \mu\text{m}$ thick should be further removed. The blue color represents positions where the milling tool removed more than originally desired, and the green color shows positions in perfect agreement. Since the hollow cylinders are almost identical, their axes and related center points are not affected. Measurement of the distances described above is therefore meaningful.

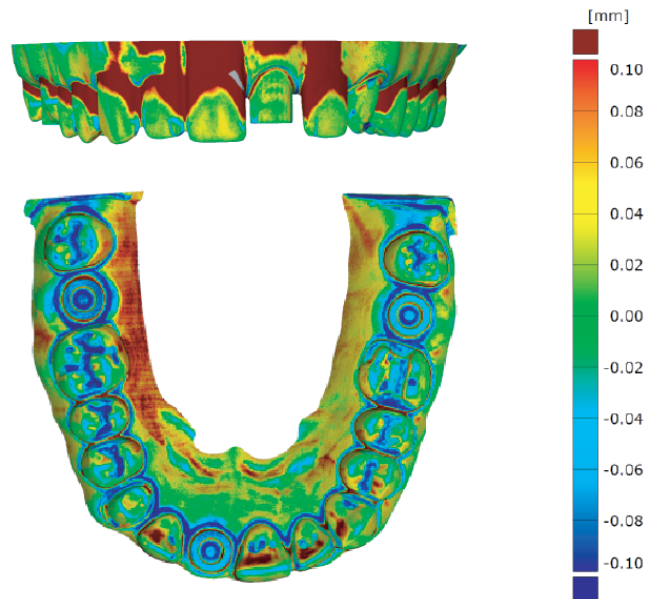


Figure 4. Three-dimensional representation of the differences between the desired geometry, given by the STL file and the data from Scan 4 and according to the color bar and the related values on the right. Perfect agreement is represented by the green color. Obviously, the milling tool provided a reasonable result, although in some areas more material than desired was removed (blue color), whilst other areas show excess material (red color). One can further observe that the hollow cylinders are larger in size than planned, but because we only consider the center points, the determination of distances is hardly affected.

3.3 Geometry of the SLA models

In specific situations, the digital workflow has to be modified, which might require a physical model to be generated from the IOS data. Here, the method of choice is stereolithography [18], but current clinical experience shows that these SLA models are less precise than conventional impressions. In order to quantify this level of precision, we produced two SLA models and used tomographic imaging and registration.

Based on the high-resolution tomography measurements performed as described above, the distances d_1 , d_2 and d_3 were extracted. For the first SLA model, the three distances corresponded to 45.611, 41.830 and 48.210 mm, whereas for the second SLA model, we found 45.753, 41.831 and 48.247 mm, meaning that the two models were not exactly the same in terms of geometry (differences were in the sub-millimeter range, see Figure 5). Comparison with STL data, however, is the benchmark. The average deviation along the full arch amounted to $(49 \pm 9) \mu\text{m}$. For the distances considered within the present study, the deviations accounted for $\Delta d_1 = 108 \mu\text{m}$, $\Delta d_2 = 154 \mu\text{m}$ and $\Delta d_3 = 18 \mu\text{m}$ (first SLA model), and $\Delta d_1 = 250 \mu\text{m}$, $\Delta d_2 = 155 \mu\text{m}$ and $\Delta d_3 = 55 \mu\text{m}$ (second SLA model). These differences between the desired design and the actual physical models clearly indicate the limitations of the stereolithography printers currently used in dental offices.

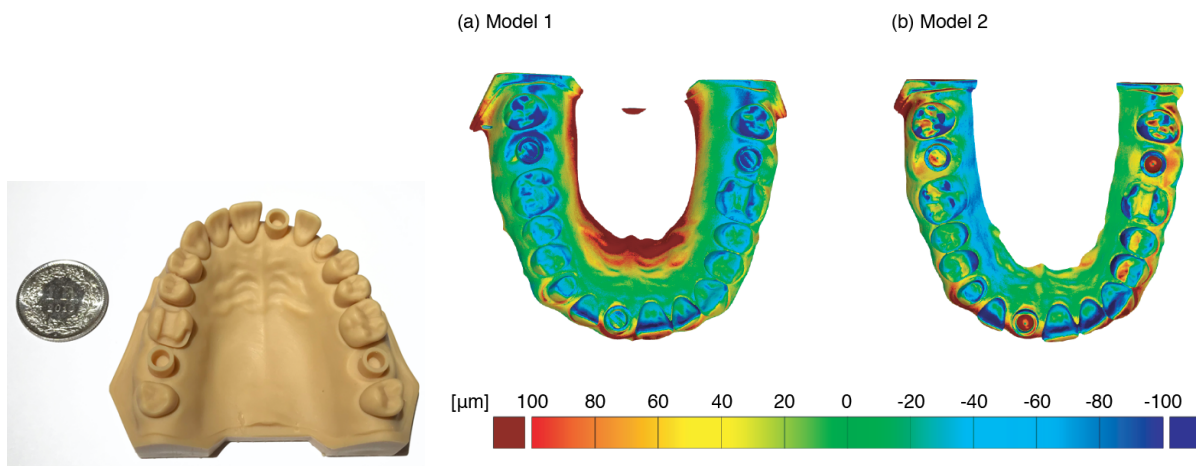


Figure 5. Three-dimensional representation of the differences between the desired geometry, given by the STL file and the high-resolution tomography data.

3.4 Accuracy of the intraoral scanners

The results obtained from the ten independent experiments with each of the IOS systems are listed in Table 1. These numbers show the reproducibility of the individual devices, when an experienced dentist has performed data acquisition according to the guidelines provided by suppliers. The data scattered within a few tens of micrometers.

In order to determine precision of the IOS systems in measuring the three selected distances, we compared these values with tomography data for the PEEK model. For the 3MTM True Definition Scanner (3M ESPE, St. Paul MN, USA), the deviations for d_1 were $(80 \pm 14) \mu\text{m}$, for d_2 $(62 \pm 8) \mu\text{m}$ and for d_3 we found $-(20 \pm 7) \mu\text{m}$. For the TRIOS[®] 3 (3shape, Copenhagen, Denmark) the length deviations amounted to $(57 \pm 18) \mu\text{m}$, $(82 \pm 16) \mu\text{m}$ and $(124 \pm 97) \mu\text{m}$, respectively. The CS 3600 (Carestream, Atlanta GA, USA) provided $(81 \pm 22) \mu\text{m}$, $(41 \pm 20) \mu\text{m}$ and $(40 \pm 64) \mu\text{m}$, respectively. Using the Medit i500 (Medit corp., Seongbuk-gu, South Korea), we found $-(93 \pm 54) \mu\text{m}$, $-(76 \pm 33) \mu\text{m}$ and $-(41 \pm 247) \mu\text{m}$. Finally, the EmeraldTM (Planmeca Oy, Helsinki, Finland) yielded $d_1 = (14 \pm 48) \mu\text{m}$, $d_2 = -(80 \pm 54) \mu\text{m}$ and $d_3 = (110 \pm 291) \mu\text{m}$. The error bars corresponded to the standard deviations derived from the ten measurements. Whereas the data were generally within a tenth of a millimeter, one recognizes some trends. The results of the Medit i500 scanner, for example, gave rise to values below the selected ground truth.

Table 1. Measured distances d_1 , d_2 and d_3 (in mm) obtained from the IOS systems used. The data determined from the microCT scans ($d_1 = 45.480$ mm, $d_2 = 41.647$ mm and $d_3 = 48.134$ mm) can be regarded as ground truth.

3M TDS			TRIOS [®] 3			CS 3600			Medit i500			EMERALD [™]		
d_1	d_2	d_3	d_1	d_2	d_3	d_1	d_2	d_3	d_1	d_2	d_3	d_1	d_2	d_3
45.577	41.695	48.118	45.536	41.749	48.256	45.567	41.703	48.128	45.458	41.607	48.036	45.439	41.665	48.144
45.545	41.708	48.111	45.548	41.728	48.106	45.519	41.698	48.027	45.440	41.627	48.120	45.499	41.512	48.349
45.534	41.711	48.094	45.568	41.721	48.244	45.564	41.707	48.185	45.456	41.573	47.907	45.411	41.528	48.192
45.535	41.693	48.035	45.53	41.729	48.279	45.536	41.658	48.147	45.391	41.568	47.857	45.499	41.537	47.891
45.559	41.707	48.001	45.563	41.723	48.309	45.568	41.673	48.202	45.405	41.567	47.705	45.479	41.594	47.887
45.567	41.726	48.122	45.538	41.723	48.287	45.550	41.676	48.157	45.380	41.562	47.62	45.484	41.527	47.874
45.574	41.719	48.190	45.514	41.715	48.088	45.593	41.679	48.194	45.357	41.55	47.595	45.490	41.575	48.472
45.568	41.709	48.188	45.524	41.745	48.274	45.572	41.677	48.219	45.349	41.576	47.499	45.578	41.506	48.424
45.573	41.718	48.160	45.519	41.705	48.338	45.580	41.686	48.243	45.316	41.502	47.449	45.552	41.597	48.561
45.568	41.705	48.122	45.534	41.756	48.403	45.559	41.725	48.235	45.317	41.576	47.430	45.510	41.628	48.645

Considering the combination of the three selected distances, one can directly compare the precision of the five IOS systems by means of the median values and the related variances. From the lowest to the highest median amplitudes, the Emerald[™] gained (2 ± 34) μm , the CS 3600 achieved (58 ± 2) μm , the 3M[™] True Definition Scanner scored (59 ± 4) μm , the TRIOS[®] 3 reached (79 ± 4) μm , and the Medit i500 led to $-(98 \pm 45)$ μm .

The average values, however, do not represent the full story. Therefore, the color-coded deviation fields are displayed in Figure 6. Although the Emerald[™] IOS reproduced the three selected distances perfectly well, the strong color gradients indicate the challenging handling and a relatively weak reproducibility. Consequently, the CS 3600, the 3M[™] True Definition Scanner and the TRIOS[®] 3 might be the better choice concerning reproducible and precise measurement within the oral cavity of the patient. The results displayed in Figure 6 also show that the Medit i500 is less precise than other IOS systems.

Using the software GOM Inspect (GOM GmbH, Braunschweig, Germany), one finds a similar result. This software provided the following precision values: TRIOS[®] 3 – 35 μm , CS 3600 – 43 μm and 3M[™] True Definition Scanner – 46 μm . The other two systems yielded less precise data: Medit i500 – 93 μm and Emerald[™] – 97 μm . If only a single quadrant is considered, one finds another picture; therefore, the selection of the best available IOS system depends on the clinical case, the training of the dentist and the convenience.

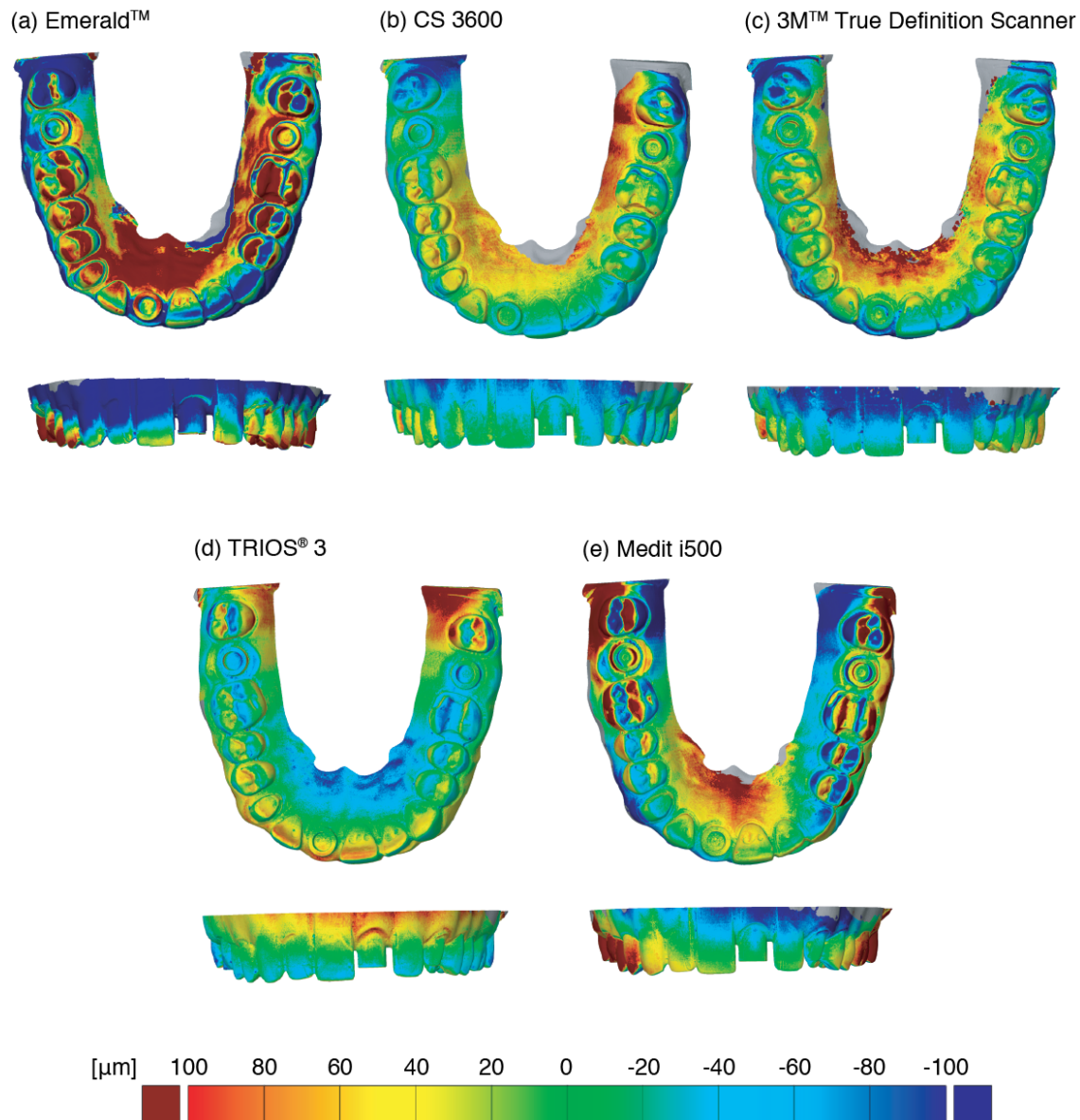


Figure 6. Color-coded deviation field of the IOS derived from the difference to the selected ground truth, i.e. the high-resolution precision tomography experiments using nanotom[®] m.

4. CONCLUSIONS

The previously scanned dental model [2] was not only captured using the nanotom[®] m, but also analyzed by a coordinate measuring machine reaching true micrometer resolution. Therefore, the precision of the nanotom[®] m study was validated. Replacing the previously used metal cast with the mechanically machined PEEK model, we were able to reduce significantly streak artifacts. Neither full dentition model included edentulous areas, which can be more difficult to scan and could have affected the results [19]. This experimental study avoided the presence of soft tissues, saliva, blood, filling materials or space limitations, which often can compromise the accuracy of the scan data in a clinical setting.

Compared to the study presented herein, it is more challenging to determine the precision of IOS systems in an *in vivo* setting. In such studies, the reference model is digitized after a conventional impression and may contain related errors.

There are only a few full-arch *in vivo* studies (see for example ref. [1] and a somehow older study [20]), but the results nevertheless correlate with our findings. physiological tooth mobility can range from 30 to 100 μm [21], and the clinically acceptable limit of the marginal gap of a crown is generally 120 μm [14].

For the full arch, the IOS systems considered herein show reasonable results, although the precision of at least some systems should be improved. In a separate quadrant, however, the devices reach the desired performance.

If the situation requires a physical model, which is then produced using stereolithography technology, full-arch accuracy is often not achieved – contrary to the conventional silicone impressions. As a consequence, they are generally considered as unsuitable for larger prosthetic reconstructions [2, 3]. In this study, we incorporated only two printers from one model, and thus, the obtained data have limited informative value.

Besides precision, there are further factors including scanning time, the learning curve or intraoral-camera size, each of which strongly affects the usability of an IOS device. Nevertheless, we can state that current digital impressions exhibit micrometer precision and generally produce clinically acceptable data. All analyzed IOS devices are suitable for generating three-dimensional data for working models, single crowns and small bridges.

Since the precision of the digital impressions is fundamental for most clinical applications and the systems differ significantly, it is preferable to use one of the more precise instruments, namely the TRIOS[®] 3, the CS 3600, and the 3M[™] True Definition Scanner for the full-arch scanning. Digital impressions have become a valuable alternative to conventional approaches.

ACKNOWLEDGEMENT

The authors thank ArteDent, Palma de Mallorca, Spain for the reference model and the SLA model production. The authors also thank the companies Kaladent AG, St. Gallen, Switzerland, Curaden Dentaldepot, Kriens, Switzerland and Alfons Stöcklin, Praxis-Team St. Margarethen, Binningen, Switzerland for providing the intraoral scanners. The financial support of the Swiss National Science Foundation in the frame of the R'equip initiative 316030_133802 is gratefully acknowledged.

REFERENCES

- [1] Ender, A., Attin, T., and Mehl, A., "In vivo precision of conventional and digital methods of obtaining complete-arch dental impressions," *J Prosthet Dent* **115**(3), 313-20 (2016).
- [2] Vögtlin, C. S., G; Jäger, K; Müller, B, "Comparing the accuracy of master models based on digital intra-oral scanners with conventional plaster casts," *Phys Med* **1**, 20-26 (2016).
- [3] Brown, G. B., Currier, G. F., Kadioglu, O., and Kierl, J. P., "Accuracy of 3-dimensional printed dental models reconstructed from digital intraoral impressions," *Am J Orthod Dentofacial Orthop* **154**(5), 733-739 (2018).
- [4] Lim, J. H., Park, J. M., Kim, M., Heo, S. J., and Myung, J. Y., "Comparison of digital intraoral scanner reproducibility and image trueness considering repetitive experience," *J Prosthet Dent* **119**(2), 225-232 (2018).
- [5] Treesh, J. C., Liacouras, P. C., Taft, R. M., Brooks, D. I., Raiciulescu, S., Ellert, D. O., Grant, G. T., and Ye, L., "Complete-arch accuracy of intraoral scanners," *J Prosthet Dent*, (2018).
- [6] Mangano, A., Beretta, M., Luongo, G., Mangano, C., and Mangano, F., "Conventional Vs Digital Impressions: Acceptability, Treatment Comfort and Stress Among Young Orthodontic Patients," *Open Dent J* **12**, 118-124 (2018).
- [7] Pradies, G., Zarauz, C., Valverde, A., Ferreira, A., and Martinez-Rus, F., "Clinical evaluation comparing the fit of all-ceramic crowns obtained from silicone and digital intraoral impressions based on wavefront sampling technology," *J Dent* **43**(2), 201-8 (2015).

- [8] Jager, K., and Vogtlin, C., "[Digital workflow with the Lava Chairside Oral Scanner C.O.S. and Lava technique]," *Schweiz Monatsschr Zahnmed* **122**(4), 307-24 (2012).
- [9] Mormann, W. H., "The evolution of the CEREC system," *J Am Dent Assoc* **137 Suppl**, 7S-13S (2006).
- [10] Zimmermann, M., Mehl, A., Mormann, W. H., and Reich, S., "Intraoral scanning systems - a current overview," *Int J Comput Dent* **18**(2), 101-29 (2015).
- [11] Mangano, F., Gandolfi, A., Luongo, G., and Logozzo, S., "Intraoral scanners in dentistry: a review of the current literature," *BMC Oral Health* **17**(1), 149 (2017).
- [12] Dolcini, G. A., Colombo, M., and Mangano, C., "From Guided Surgery to Final Prosthesis with a Fully Digital Procedure: A Prospective Clinical Study on 15 Partially Edentulous Patients," *Int J Dent* **2016**, 7358423 (2016).
- [13] Nedelcu, R., Olsson, P., Nystrom, I., Ryden, J., and Thor, A., "Accuracy and precision of 3 intraoral scanners and accuracy of conventional impressions: A novel in vivo analysis method," *J Dent* **69**, 110-118 (2018).
- [14] Ahlholm, P., Sipila, K., Vallittu, P., Jakonen, M., and Kotiranta, U., "Digital Versus Conventional Impressions in Fixed Prosthodontics: A Review," *J Prosthodont* **27**(1), 35-41 (2018).
- [15] Imburgia, M., Logozzo, S., Hauschild, U., Veronesi, G., Mangano, C., and Mangano, F. G., "Accuracy of four intraoral scanners in oral implantology: a comparative in vitro study," *BMC Oral Health* **17**(1), 92 (2017).
- [16] Rzanny, A. G., R., Nietzsche, S., and Küller, H., "PEEK: Werkstoffkundliche Eigenschaften – mit Blick auf die dentale Anwendung," *ZTM* **2**, 102-110 (2017).
- [17] Althaus, J., Urwyler, P., Padeste, C., Heuberger, R., Deyhle, H., Schiff, H., Gobrecht, J., Piele, U., Scharnweber, D., Peters, K., and Müller, B., "Micro- and nanostructured polymer substrates for biomedical applications," *Proc SPIE* **8339**, 83390Q (2012).
- [18] Rebong, R. E., Stewart, K. T., Utreja, A., and Ghoneima, A. A., "Accuracy of three-dimensional dental resin models created by fused deposition modeling, stereolithography, and Polyjet prototype technologies: A comparative study," *Angle Orthod* **88**(3), 363-369 (2018).
- [19] Flugge, T. V., Att, W., Metzger, M. C., and Nelson, K., "Precision of Dental Implant Digitization Using Intraoral Scanners," *Int J Prosthodont* **29**(3), 277-83 (2016).
- [20] Brogle-Kim, Y.-C., Deyhle, H., Müller, B., Schulz, G., Bormann, T., Beckmann, F., and Jäger, K., "Evaluation of oral scanning in comparison to impression using three-dimensional registration," *Proc SPIE* **8506**, 85061R (2012).
- [21] Castellini, P., Scalise, L., and Tomasini, E. P., "Teeth mobility measurement: a laser vibrometry approach," *J Clin Laser Med Surg* **16**(5), 269-72 (1998).